Pulsed EPR and Ab Initio Calculation on $[Ni(CN)_4]^{3-}$ in NaCl and KCl Host Lattices

A. A. Leitão,† J. A. Coelho Neto,‡ N. M. Pinhal,‡ C. E. Bielschowsky,† and N. V. Vugman*,‡

Instituto de Física and Instituto de Química, Universidade Federal do Rio de Janeiro, Rio de Janeiro, RJ, Brazil, 21910-240

Received: June 20, 2000; In Final Form: October 30, 2000

Paramagnetic $3d^9$ $[Ni(CN)_4]^{3-}$ complexes, with the unpaired electron in a $d_{x^2-y^2}$ orbital, have been generated from diamagnetic Ni(II) $3d^8$ cyanide complexes in KCl or NaCl host lattices. The magnetic and quadrupolar hyperfine interactions with the four ^{14}N, hidden in the CW-EPR (continuous wave electron paramagnetic ressonance) line width, are revealed by pulsed EPR and ENDOR (electron nuclear double resonance) angular variation studies. Ab initio embedded UMP2 cluster calculations, which take into account short- and long-range crystal interactions, confirm the unpaired electron orbital assignment and are in agreement with the measured hyperfine values. The trend of ^{14}N A_{iso} values (7.7 MHz for NaCl and 6.8 MHz for KCl) is given by the Ni−CN distance, modified in each host lattice. Small asymmetry factors (about 0.04) for the ^{14}N quadrupolar tensor are obtained both in experiment and in theory. The experimental lines and the calculations indicate spin density at the cations of both lattices. Experimental and theoretical data indicate that lattice chlorine ions near the Ni atom, in axial positions, are not chemically coordinated to Ni. Spin density on these ions arises only from spin polarization of their valence orbitals and of the valence orbitals of the complex.

Introduction

Transition metal cyanide compounds are important in many aspects of modern chemistry. Insertion of these complexes in ionic fcc host lattices, at low concentration, provides an interesting way to study their paramagnetic coordination complexes.[1−4] The complexes, stabilized in the host lattices, are oriented toward the principal crystal axes. Furthermore, dilution minimizes intermolecular interactions.

In the past few years, progress has been attained both experimentally and theoretically in the study of such systems, allowing a detailed explanation of the electronic structure and related properties. On the experimental side, the resolution improvement via electron spin−echo envelope modulation (ESEEM) and electron nuclear double ressonance (ENDOR) measurements reveals small hyperfine interactions hidden in the line width of the tradicional continuous wave (CW) experiments.[5]

On the theoretical side, progress has been attained concerning the representation of the crystalline environments[6−12] for different purposes, as, for example, electronic spectroscopic and hyperfine interaction calculations in ionic pure or impure crystals. Embedded cluster calculations (ECC)[6−15] proved to be an important tool in the determination of electronic structure and properties for systems in crystals where a precise wave function is needed in a localized spatial region. For this purpose, total ion potentials (TIP)[10,11] may be used to take into account short-range interactions and Evjen point charge procedure[16] to take into account the long-range interactions. In particular, an accurate determination of the geometry of molecular impurities in crystal host lattices, not achievable by X-ray diffraction spectroscopy or by other experimental methods, has been obtained by such methodology.

In what concerns the calculation and interpretation of hyperfine coupling for gas-phase isolated radicals,[17−20] the importance of spin-polarization and correlation effects has been revealed. For this purpose, unrestricted Hartree−Fock (UHF) and Moller−Plesset perturbation theory[21] based on ab initio unrestricted spin Hartree−Fock (UMP2) have provided theoretical results in excellent agreement with the experiments.[19]

In this paper we report accurate theoretical and experimental results for $[Ni(CN)_4]^{3-}$ complex in cubic NaCl or KCl host lattices. This square planar paramagnetic complex can be formed by radiation damage on face centered cubic host lattices such as NaCl or KCl doped with the $[Ni(CN)_4]^{2-}$ anion.[1,2] In this situation, electron paramagnetic resonance (EPR) spectroscopy reveals that the complex electronic ground state has a B_{1g} symmetry (unpaired electron in a $d_{x^2-y^2}$ orbital).

Some previous works suggest that the nature of the coordination bonds of complexes are independent of the host lattice and that the distance between metal and CN is affected by the ionic interactions with the crystal.[4] Also, the electric field generated at the complex by a host lattice influences the splitting of the central Ni atom d orbitals as well as the CN ligands π orbitals. A square planar impurity like $[Ni(CN)_4]^{3-}$ in KCl or NaCl host lattices has two Cl^- ions as first neighbors of the Ni atom. ESEEM experiments show hyperfine interactions with the nuclei of these anions. The degree of participation of these host ions on the molecular structure of the complex and the influence of crystal structure on measured molecular properties are questions that we investigate in this work.

Direct comparison between theoretical and experimental data can be made for isotropic magnetic hyperfine couplings (A_{iso}) and the quadrupole tensor. It is possible to perform a qualitative comparison between the calculated ground state and the measured **g** tensor, since this tensor is related to the symmetry of the unpaired electron wave function.[1,2]

We performed accurate ESEEM and ENDOR measurements of magnetic and quadrupolar hyperfine interactions with the four

* Corresponding author. E-mail: ney@if.ufrj.br.
† Instituto de Química.
‡ Instituto de Física.

10.1021/jp002208c CCC: $20.00
Published on Web 12/29/2000

^{14}N in paramagnetic $3d^9$ $[Ni(CN)_4]^{3-}$ complexes in KCl and NaCl host lattices. The magnetic and quadrupolar hyperfine tensors, hidden in the continue wave (CW) EPR line width,[1,2] are revealed by ENDOR and ESEEM angular variation studies. Lines attributed to ^{23}Na, ^{39}K, ^{35}Cl, and ^{37}Cl were observed in ESEEM experiments. In particular, interpretation of ^{23}Na lines shows some spin density at these host ions.

The geometry, electronic structure, and isotropic hyperfine interaction (A_{iso}) of $[Ni(CN)_4Cl_2]^{5-}$ cluster in KCl and NaCl host lattices are determined by ab initio embedded cluster calculations (UMP2[22] calculations), which are compared with UHF and ROHF calculations. The present theoretical results, besides confirming the unpaired electron orbital assignment and providing precise localization of cyanides and axial host chlorines, are in excellent agreement with the measured properties for both host lattices.

Experimental Section

Cubic single crystals of KCl or NaCl doped with 0.5% M proportion of $K_2Ni(CN)_4$ were grown by slow evaporation of a saturated aqueous solution and submitted to 80 kV X-ray irradiation in order to create paramagnetic centers. Both reduced d^9 and oxidized d^7 paramagnetic species are formed.[1,2] Substitution of a cluster $[KCl_4]^{3-}$ or $[NaCl_4]^{3-}$ by the anion $[Ni(CN)_4]^{2-}$ creates a charge-compensating cation vacancy. Gain or loss of an electron creates the reduction or oxidation products of the dopants.

Pulsed EPR experiments were performed at the X-band (9.724 GHz) on a Bruker ESP380E CW/FT spectrometer equipped with a dielectric cavity inserted into an Oxford CF-935 variable temperature cryostat at 16 K. The stimulated echo was optimized by power variation of a sequence of three 16 ns pulses. ESEEM spectra were obtained as a result of a sum projection of a 512 $\times$ 256 2D spectrum, varying the distances between the second (F1 domain) and the third pulses (F2 domain) with a 8 ns step. The cubic crystals were mounted on a small Teflon cylinder into a quartz tube. The crystal was rotated about one of the principal axes so that both parallel and perpendicular spectral features could be obtained by a 90° rotation. Angular variation studies were performed with the help of a homemade goniometer, calibrated in tenths of degrees.

ENDOR measurements were made at 10 K in a Bruker ESP300 spectrometer equipped with an ENDOR module and an Oxford CF-935 variable temperature cryostat, at 9.423 GHz using 6.3 mW microwave power and 177 kHz modulation depth for the radio frequency sweep.

Experimental Results

Separation between the two occurring paramagnetic species was based on their distinct spin−lattice relaxation times, T_1. Adequate choice of experimental repetition rates and temperature leads to selective saturation of the d^7 species, as shown in Figure 1. In this way, all ESEEM spectra were taken at a repetition rate such that the undesired d^7 species was almost completely saturated. Measured g values for the d^9 species are $g_{||} = 2.108$ and $g_{\perp} = 2.041$.

A typical ESEEM spectrum in the frequency domain for reduced $3d^9$ $[Ni(CN)_4]^{3-}$ complexes in NaCl host lattice is shown in Figure 2. The applied magnetic field was aligned to the complex principal symmetry axis (parallel position, $\theta = 0$). Lines symmetrically located around the sodium nuclear Zeeman frequency and around nuclear Zeeman frequencies of the 35 and 37 chlorines isotopes are clearly seen, besides lines attributed to interaction between the unpaired electron and the four nitrogens. Numerous ^{14}N lines indicate the presence of a quadrupolar interaction. Furthermore, there is also the presence of spurious second harmonic lines. A comparison between ESEEM spectra for $[Ni(CN)_4]^{3-}$ in NaCl and KCl lattices, taken at the parallel and the perpendicular positions, is shown in Figure 3. Despite the fact that the KCl host crystals were larger, spectra with better signal-to-noise ratios were obtained with the NaCl crystals. This may indicate that the concentration of paramagnetic centers was larger in the NaCl host.

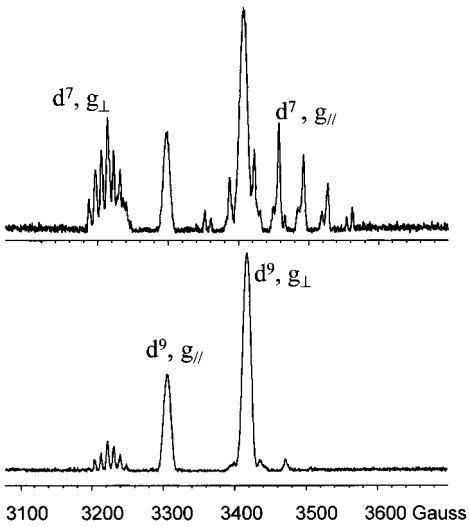

Figure 1. Selection of species by spin lattice relaxation times in echo-induced EPR of irradiated $K_2Ni(CN)_4$ in NaCl host lattice: (top) 3 ms repetition rate at 50 K and (bottom) 2 ms repetition rate at 16 K.

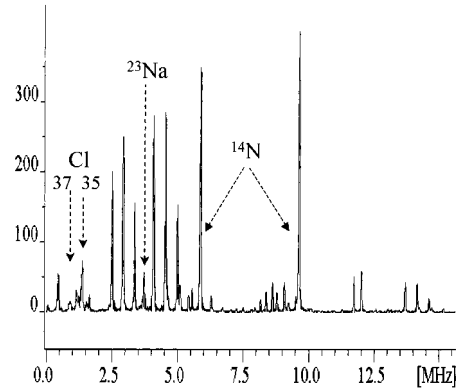

Figure 2. Three-pulse frequency domain absolute valued ESEEM spectrum of $3d^9$ $[Ni(CN)_4]^{3-}$ species in NaCl host lattice at 16 K. The stimulated echo was optimized by power variation of a sequence of three 16 ns pulses. ESEEM spectra were obtained as a result of a sum projection of a 512 $\times$ 256 2D spectrum, varying the distances between the second (F1 domain) and the third pulses (F2 domain) with a 8 ns step. Arrows point to the sodium and chlorine matrix lines and to the strongest nitrogen lines.

To identify lines to nitrogen multiplets, we perfomed a 2D-ESEEM study in the parallel and perpendicular positions (Figure 4). Clear line correlations can be obtained from Figure 4, providing a starting point for spectrum interpretation. Six lines may show up when quadrupolar effects are present. The ESEEM dependence on ^{14}N quadrupolar interaction was explored on the basis of the MAGNSPEC[23] program's numerical calculations. The highest frequency line is practically insensitive to quadrupolar interaction. As a consequence, once this line is identified, a preliminary value for the magnetic hyperfine coupling can be measured. Finer details of the spin Hamiltonian tensors may only be revealed by a complete angular variation study, as shown in Figure 5. Laborious fitting with the MAGNSPEC program

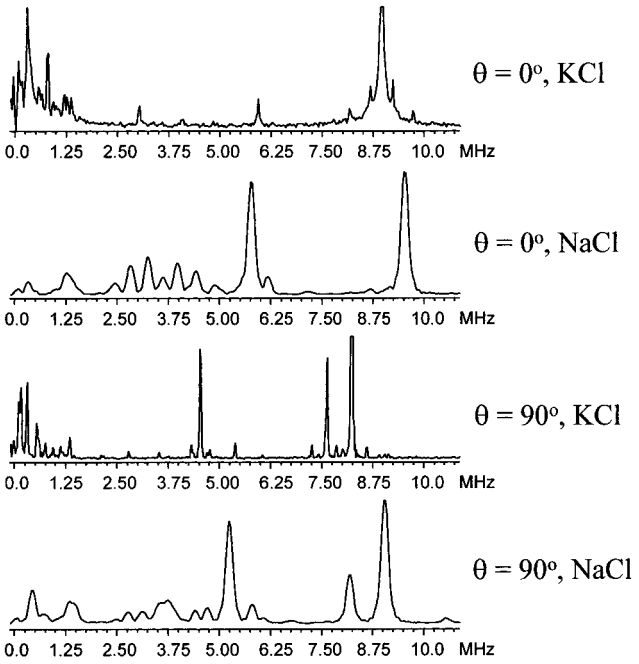

Figure 3. Comparison among three-pulse absolute value FT spectra of $3d^9$ $[Ni(CN)_4]^{3-}$ species in NaCl and KCl host lattices at 16 K, at the parallel ($\theta = 0°$) and perpendicular ($\theta = 90°$) positions with respect to the external magnetic field. Lines in NaCl are broader because memory phase times are smaller for this host lattice as compared to KCl.

leads to a best agreement with experimental data when we use the spin Hamiltonian parameters shown in Tables 1 and 2. It is interesting to notice from this figure that a predicted line at 6.3 MHz is systematically missing from ESEEM experimental data. This line corresponds to a low-probability branching transition.

ENDOR angular variation studies (Figure 6) reproduce the ESEEM angular variation and provide complementary information. The line missing in the ESEEM spectra is now clearly seen, since ENDOR lines are not sensitive to branching transitions.

ESEEM lines corresponding to host lattice ions can be easily found. For the complex in NaCl host lattice, ^{23}Na lines are found partially superposed to ^{35}Cl, ^{37}Cl, and ^{14}N lines. Interpretation of these lines (see Figure 7), using the MAGNSPEC program, suggests three distinct interacting Na^+ host lattice ions: (i) the so-called matrix ions (distant but still interacting), with lines at 3.86 MHz (perpendicular) and 3.74 MHz (parallel), signed with arrows in the figure; (ii) second neighbors to Ni atom (12 ions), lines signed by rectangles in this figure; and (iii) fourth neighbors to Ni atoms near the cyanides (4 ions), lines signed by ellipses (see also Figure 8).

Lines due to ^{19}K are mixed to ^{35}Cl, ^{37}Cl lines in the ESEEM spectrum of $[Ni(CN)_4]^{3-}$ in KCl host lattice, making interpretation rather difficult. Spectrum interpretation is also difficult for ^{35}Cl, ^{37}Cl lines themselves, both in NaCl and KCl host lattices, as these lines are weak and superposed to other lines. Assignments have been done in these cases using the UMP2 theoretical results for A_{iso} presented in the next section and a point dipole approximation for the dipolar interaction (A_{dip}).

Theoretical Methods and Discussion

The system under study is represented by an $[Ni(CN)_4Cl_2]^{5-}$ cluster (the central Ni and its neighboring atoms), added by 18 total ion potentials (TIP)[10,11] representing the surrounding K^+ or Na^+ ions, as shown in Figure 8, and by 1306 point charges,[16]

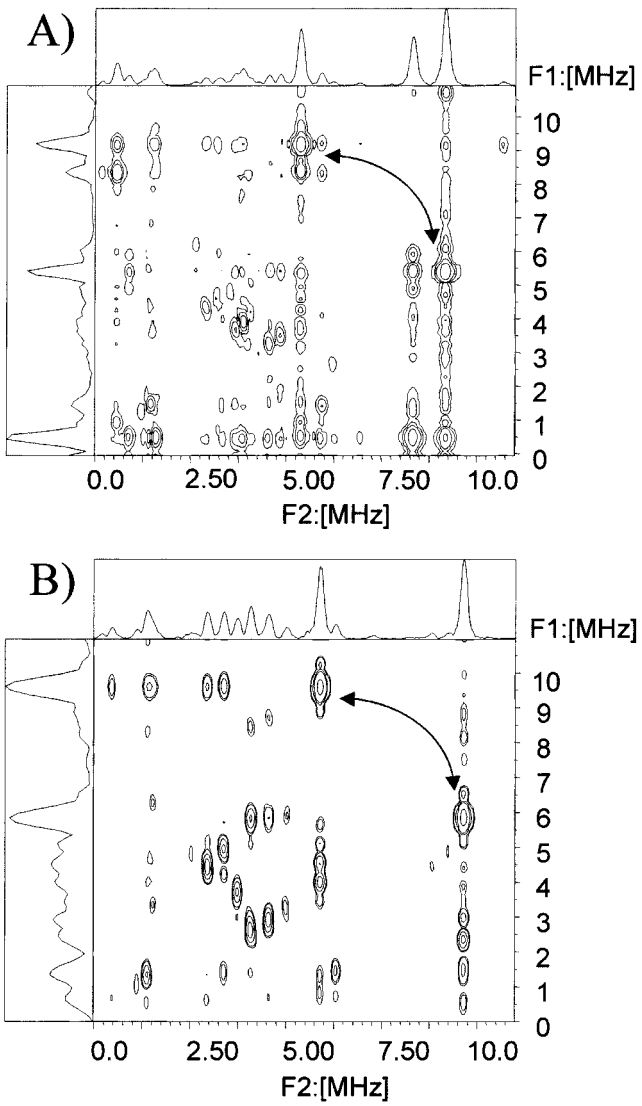

Figure 4. Parallel (A) and perpendicular position (B) 512 × 256 8 ns step 2D-ESEEM contour plots of the $3d^9$ $[Ni(CN)_4]^{3-}$ species in NaCl host lattice at 16 K, obtained after line base correction, apodization, zero filling, FFT along the F2 axis, absolute value, FFT along the F1 axis, and absolute value. The stimulated echo was optimized by power variation of a sequence of three 16 ns pulses. Arrows exemplify nitrogen correlated lines. Sodium correlated lines occupy the center of the plots.

representing the rest of the crystal. A 6-31+G* Gaussian basis set was used for the N, C, and Cl atoms, and a LanL2DZ[24] basis set was used for the central metal. This basis includes polarization and diffuse functions, needed to properly describe delocalized valence electrons of the complex bonding. The 18 electrons of K^+ ions or the 10 electrons of Na^+ that surround the $[Ni(CN)_4Cl_2]^{5-}$ cluster are represented by effective core potentials[24] for the core of K and Na neutral atoms. They take into account the short-range potentials acting on the quantum-mechanical cluster due to the infinite crystal. The long-range Coulombic potential of the infinite crystal was considered through point charges. At the borders of the cube, ionic fractional charges were used following the Evjen procedure[16] in order to increase convergence of the Madelung potential at the cluster and to preserve system neutrality. The point charges and TIPs are placed in positions corresponding to pure crystal lattices. With the cluster, the TIPs, and the point charges, a cube with an edge composed by 11 point charges is established.

Electronic structure and the optimal geometry of the complex were determined by UMP2 calculations using all valence and

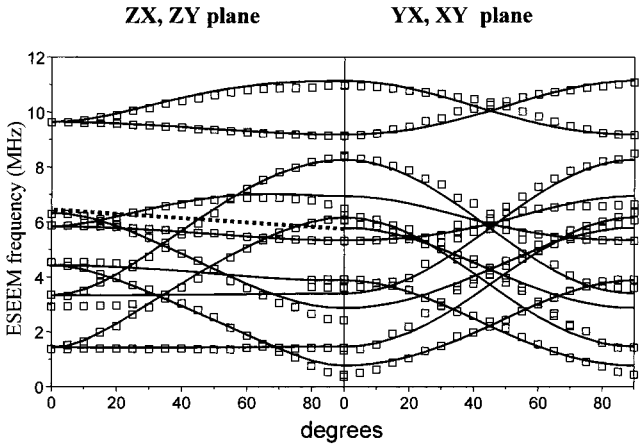

Figure 5. Angular variation of ^{14}N ESEEM lines for the $3d^9$ $[Ni(CN)_4]^{3-}$ species in NaCl host lattice at 16 K for the *zx*, *zy*, *yx*, *xy* planes. Experimental points and errors are indicated by squares. Solid curves refer to MAGNSPEC fitting. The broken curve corresponds to a predicted but not observed line.

TABLE 1: Measured Components of A Tensor for ^{14}N Atoms at $[Ni(CN)_4]^{3-}$ Complex (MHz)

host	A_x	A_y	A_z
NaCl	7.25	6.65	9.04
KCl	6.6	5.9	8.0

TABLE 2: Calculated and Measured Quadrupolar Interactions in MHz

	NaCl host lattice			KCl host lattice		
atom	P_x	P_y	P_z	P_x	P_y	P_z
Theoretical Results (UMP2)						
N[a]	−0.78	−0.72	1.51	−0.74	−0.69	1.43
Cl[b]	0.11	0.11	−0.22	0.11	0.11	−0.22
Experimental Results						
N[a]	−1.00	−0.80	1.80	−0.9	−0.8	1.7

[a] The *z* axis coincides with the CN axis, *y* is parallel to the complex principal symmetry axis, and *x* axis is orthogonal to the *yz* plane. [b] As shown in Figure 8.

virtual orbitals. The distance C−N was kept[25] as 1.15 Å and the Ni−C and Ni−Cl distances were optimized. Positions of TIPs and point charges were kept constant. Hyperfine quadrupolar and magnetic interactions were calculated using the same method.

The A_{iso} couplings were calculated by multiplying the evaluated spin density[19,20] $\rho(N)$ at nucleus N by the nuclear (g_N) and electronic (g) g-factors, the Bohr magneton (β), the nuclear magneton (β_N):

$$A_{iso}{}^N = \frac{8\pi}{3} g\beta g_N \beta_N \rho(N)$$

To analyze the distinct contributions to the hyperfine interactions, restricted open-shell Hartree−Fock (ROHF) and unrestricted spin Hartree−Fock (UHF) wave functions were calculated at the equilibrium geometry.

The hyperfine quadrupolar coupling tensor was calculated from the expression[18]

$$P_{N,i} = \frac{eQ_N EFG_{N,i}}{2I_N(2I_N - 1)}$$

where e, I_N, Q_N, $EFG_{N,i}$ are respectively the electron charge, the nuclear spin, the nuclear quadrupole momentum, and the

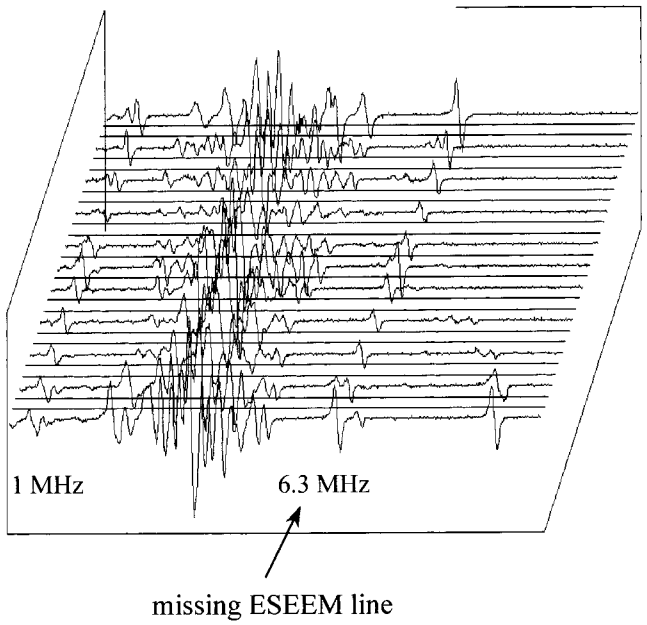

Figure 6. $[Ni(CN)_4]^{3-}$ in NaCl host lattice at 10 K CW-ENDOR angular variation from the parallel to the perpendicular position. Notice the almost isotropic line at 6.3 MHz, missing in the ESEEM spectra.

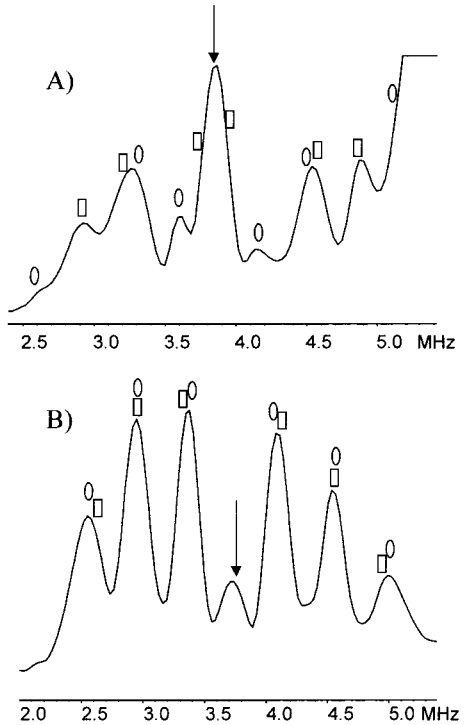

Figure 7. ^{23}Na ESEEM spectrum: (a) perpendicular and (b) parallel. The arrow points to the ^{23}Na matrix line, rectangles correspond to Ni second neighbors, and ellipses correspond to Ni fourth neighbors, near the cyanides (see Figure 8).

electric field gradient at nucleus N. Index i denotes x, y, or z components. The asymmetry factor using experimental or theoretical values can be calculated with quadrupolar components:

$$\eta = \frac{P_x - P_y}{P_z}$$

The Gaussian 94 program[26] was used to perform theoretical calculations. The $\langle S^2 \rangle$ values for the calculated UHF wave

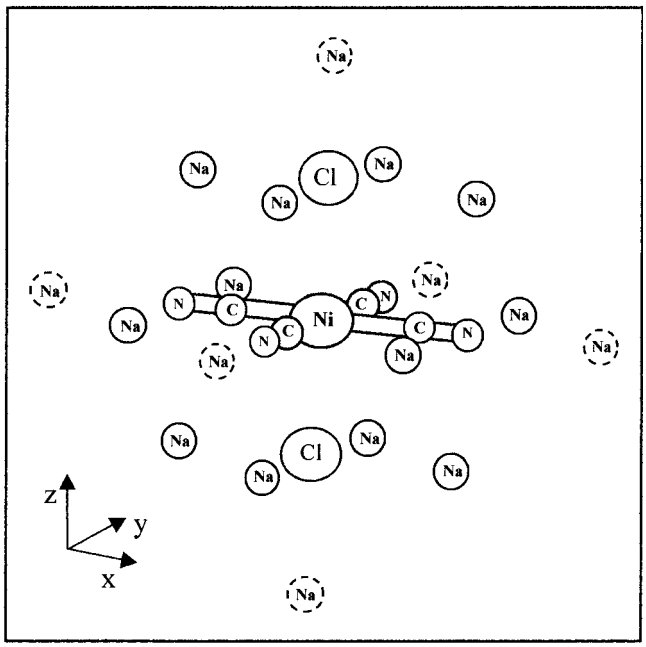

Figure 8. Scheme of the complex $[Ni(CN)_4]^{3-}$ with some neighbors in NaCl host lattice. The Na ions as second neighbors to Ni atom are represented with firm lines and the Na ions as fourth neighbors to Ni atom with segmented lines.

TABLE 3: Calculated Equilibrium Geometric Parameters for the Cluster $[Ni(CN)_4Cl_2]^{5-}$ by UMP2 Method (Å)

geometric parameter	NaCl host lattice	KCl host lattice
distance NiCl	2.90	3.23
distance NiC	2.03	2.11
distance NiN	3.18	3.26
distance CN	1.15	1.15
interatomic distance for the perfect crystal[a]	2.82	3.15

[a] Reference 27.

functions are 0.7619 and 0.7597 for NaCl and KCl host lattices. The $\langle S^2 \rangle$ values for the UMP2 wave functions are 0.7568 and 0.7556, respectively, for NaCl and KCl host lattices. These $\langle S^2 \rangle$ values, close to the correct value 0.75, indicate a negligible influence of the spin contamination in the calculated properties.[22]

The calculated electronic structure assigns B_{1g} symmetry to the unpaired electron orbital, in agreement with the measured g values ($g_{\parallel} > g_{\perp} > 2.0023$).[1,2] The orbital has an antibonding character, as a function of the nodes between the Ni atom and the cyanides ligands.

Table 3 shows that the distances between Ni and Cl atoms are close to the lattice constants for the perfect crystals. We assume that there is no covalent bonding between the metal and the two axial Cl atoms. This assumption is justified considering that the calculated Mulliken charge on chlorine atoms is -0.93 and the nonbonding character of the molecular orbitals that is localized on Cl ions. The small values for the calculated quadrupolar interactions (Table 2) indicate cubic symmetry around these ions, as expected for host chlorines.

Table 2 also shows the calculated values for the quadrupolar tensor, in good agreement with experimental data for ^{14}N atoms. The small difference between the values of ^{14}N quadrupolar components in the two host lattices is a consequence of the Ni−N distance once the host lattice contritbutes to EFG. We can see in Table 2 that the modulus of ^{14}N quadrupolar components is higher for NaCl than for the KCl host lattice. Table 3 shows the difference between the Ni−N distance and the lattice constant to be 0.36 and 0.11 for the NaCl and KCl hosts, respectively.

TABLE 4: A_{iso} for the $[Ni(CN)_4]^{3-}$ Complex and Nearest Host Ions, in MHz

	NaCl host lattice				KCl host lattice			
atom	ROHF	UHF	UMP2	expl[a]	ROHF	UHF	UMP2	expl[a]
^{14}N	2.3	2.2	8.3	7.7	1.7	1.6	6.6	6.8
^{13}C	37.3	64.4	78.4	−	29.9	52.3	62.0	105[b]
^{35}Cl	0.0	−2.5	−4.1	>(−5)	0.0	−1.7	−2.6	>(−4)
^{23}Na[c]	*d*	*d*	*d*	0.33				
^{23}Na[e]	*f*	0.40	0.19	0.17				

[a] $A_{iso} = (A_x + A_y + A_z)/3$. [b] Reference 1. [c] Na^+ ions second neighbors to Ni atom (12 ions). [d] Cluster too large to the present computational capabilities. [e] Na^+ ions fourth neighbors to Ni atom near cyanides calculated with a cluster $[Na_4Ni(CN)_4Cl_2]-$. [f] Convergence not acquired in the calculations.

The corresponding asymmetry factors (η), calculated from theoretical results for ^{14}N quadrupolar interactions, are 0.040 and 0.034, close to the experimental values. These small values suggest a high similarity between π_x and π_y orbitals at the cyanides, justifying the small hyperfine anisotropy found in the experiments (see Table 1). This interpretation is consistent with the ESEEM ^{23}Na lines found in Figure 7, where we assign only one kind of ^{23}Na second neighbor to the Ni atom, suggesting that orbitals d_{xy}, d_{yz}, and d_{xz} at the central Ni are similar, with respect to its spin polarization and spatial distribution, to an octahedral situation. Once the complex has D_{4h} symmetry, we can infer that the electrostatic potential at the Ni site has a relevant contribution from the axial host lattice chlorine ions, leading to an effective almost octahedral symmetry for this potential.

Table 4 presents the experimental and calculated isotropic hyperfine coupling constants for ^{13}C, ^{14}N, ^{23}Na, and ^{35}Cl atoms at the optimized geometry. Three distinct methods were used for A_{iso} calulations: the ROHF method, which does not consider spin-polarization or correlation effects; the UHF method, which considers spin-polarization effects; and the UMP2 method, which takes into account both spin-polarization and part of the correlation effects. This table clearly indicates that both spin-polarization effects, estimated from the difference between ROHF and UHF results, and correlation effects, estimated from the difference between UHF and UMP2 results, are essential to appropriately describe the isotropic hyperfine coupling constants A_{iso}. That is consistent with previous works with complexes[12] and small radicals.[19]

Table 4 shows that the difference between theoretical and experimental ESEEM A_{iso} values for ^{14}N is less than 10%. Both theory and CW EPR experiments predict small values for A_{iso} for Cl atoms as first neighbors to Ni atoms. The ESEEM spectra for the $[Ni(CN)_4]^{3-}$ complex in NaCl and KCl host lattices present lines that can be attributed to chlorines, in agreement with the A_{iso} values calculated by the UMP2 method. For symmetry reasons there is no contribution from the unpaired electron b_{1g} orbital to the spin density at the Cl−Ni−Cl axis. The ^{35}Cl A_{iso} values can be understood by the spin polarization of valence orbitals.[12] Comparison between axial ^{35}Cl A_{iso} null values calculated by ROHF and nonnull values calculated by UHF (Table 4) confirms that the spin density at these nuclei results from spin polarization of the complex and chlorine ions valence orbitals.

The calculations give the correct trend for ^{14}N A_{iso} as a function of the host lattice; the value for NaCl is slightly larger than that for the KCl crystal. The optimized geometry (Table 3) explains this trend, since the Ni−C distance for NaCl host

is smaller than that for KCl, making the ^{14}N atoms in the NaCl crystal more sensitive to the unpaired electron.

A larger A_{iso} difference (around 40%) is observed between our theoretical results for ^{13}C and early experimental results using 70% ^{13}C enriched samples in KCl host lattice.[1] The difference between our calculated values and the experimental data is very probably due to difficulties in getting precise spin Hamiltonian parameters from a complex and rather superimposed CW EPR spectrum.

A_{iso} values were calculated for the ^{23}Na fourth neighbors of Ni near the cyanides in a $[Na_4Ni(CN)_4Cl_2]^-$ cluster (see Figure 8) using the UMP2 method. Good agreement between UMP2 results and experimental values is shown in Table 4. This reinforces the interpretation of the experimental ESEEM data for ^{23}Na (Figure 7), as commented in the Experimental Results section.

Conclusions

In this work we performed electron spin−echo envelope modulation (ESEEM), electron nuclear double ressonance (ENDOR) measurements, and embedded cluster ab initio UMP2 calculations for $[Ni(CN)_4]^{3-}$ complex in cubic NaCl and KCl host lattices.

The calculated final symmetry for the electronic wave function, B_{1g}, agrees with the experimental predictions inferred from the g tensor. UHF calculations indicate that the unpaired electron lies basically in a Ni $d_{x^2-y^2}$ orbital, with antibonding character.

Calculations of hyperfine magnetic and quadrupolar interactions required the UMP2 method, emphasizing the importance of polarization and correlation effects. Experimental and theoretical data indicate that lattice chlorine ions near the Ni atom, in axial positions, are not chemically coordinated to the Ni atom, behaving as host lattice ions. Spin density at these ions arises only from spin polarization of valence orbitals.

The electrostatic potential from chlorine ions and from cyanides influences the d_{xy}, d_{zx}, and d_{zy} orbitals splitting like an almost octahedral symmetry. The small spin density at the host lattice cations presents this same symmetry.

Both experimental and theoretical data for this D_{4h} system show a correlation between the very small ^{14}N quadrupole asymmetry factor and the small A_x - A_y difference in the ^{14}N magnetic hyperfine tensor, suggesting that the π_x and π_y cyanide orbitals are very simillar. The small difference between ^{14}N A_{iso} in the two host lattices is understood in terms of small differences in the Ni−C distances, imposed by the respective crystal.

The electronic structure calculated through embedded cluster UMP2 calculations shows a picture in excellent agreement with the experimental results. The approximations, Evjen for long-range lattice interactions and TIPs for short-range lattice interaction, and frozen lattice ions positions can be used to predict geometrical distortions on complexes inserted in ionic host lattices.

Acknowledgment. This work was co-sponsored by FINEP and FUJB-UFRJ. The authors are indebted to CNPq for a research fellowship (N.V.V., C.E.B.) and for CAPES for a PhD fellowship (A.A.L.).

References and Notes

(1) Zanette, S. I.; Caride, A. O.; Danon, J. *J. Chem. Phys.* **1976**, *64*, 3381.
(2) Jain, S. C.; Reddy, K. V.; Gupta, C. L.; Reddy, T. Rs. *Chem. Phys. Lett.* **1973**, *21*, 150.
(3) Pinhal, N. M.; Vugman, N. V. *J. Phys. C: Solid State Phys.* **1985**, *18*, 6273.
(4) Vugman, N. V.; Amaral, M. R., Jr. *Phys. Rev. B* **1990**, *42*, 9837.
(5) Schweiger A. *Structure Bond* **1982**, *51*, 1.
(6) Sousa, C.; Casanovas, J.; Rubio, J.; Illas, F. *J. Comput. Chem.* **1993**, *14*, 680.
(7) Aachi, J.-I.; Kosugui, N. *Bull. Chem. Soc. Jpn.* **1993**, *66*, 3314.
(8) Miyoshi, E.; Miyake, Y.; Katsuki, S.; Sakai, Y. *J. Mol. Struct.* (THEOCHEM) **1998**, *451*, 81.
(9) Berrondo, M.; Rivas-Silva, J. F. *Int. J. Quantum Chem.* **1995**, *29*, 253.
(10) Winter, N. W.; Pitzer, R. M.; Temple, D. K. *J. Chem. Phys.* **1987**, *87*, 2945.
(11) Winter, N. W.; Pitzer, R. M.; Temple, D. K. *J. Chem. Phys.* **1987**, *86*, 3549.
(12) Leitão, A. A.; Vugman, N. V.; Bielschowsky, C. E. *Chem. Phys. Lett.* **2000**, *321*, 269.
(13) Vail, J. M.; Emberly, E.; Lu, T., Gu, M.; Pandely, R. *Phys. Rev. B* **1998**, *57*, 764.
(14) Al-Abdalla, A.; Barandiarán, Z.; Seijo L.; Lindh, R. *J. Chem. Phys.* **1998**, *108*, 2005.
(15) Puchin, A. A. V.; Puchin, V. E.; Kotomin, E. A.; Reichling, M. *Sol. Stat. Comm.* **1998**, *106*, 285.
(16) Evjen, H. M. *Phys. Rev.* **1932**, *39*, 675.
(17) Chipman, D. M.; Carmichael, I.; Feller, D. *J. Phys. Chem.* **1991**, *95*, 4702.
(18) Penner, G. H. *Chem. Phys. Lett.* **1996**, *261*, 665.
(19) Gauld, J. W.; Eriksson, L. A.; Radom, L. *J. Phys. Chem. A* **1997**, *101*, 1352.
(20) Knight, L. B., Jr; Hill, D.; Berry, K.; Babb, R.; Feller, D. *J. Chem. Phys.* **1996**, *105*, 5672.
(21) Møller, Chr; Plesset, M. S. *Phys Rev* **1934**, *46*, 618.
(22) Chen W.; Schlegel, H. B. *J. Chem. Phys.* **1994**, *101*, 5957.
(23) Mackey, J. H.; Kopp, M.; Tynan, E. C.; Yen, Teh Fu in ESR of Metal Complexes, Plenum: New York, 1969; p 33.
(24) Hay, P. J.; Wadt, W. R. *J. Chem. Phys.* **1985**, *82*, 270; Wadt, W. R.; Hay, P. J. *J. Chem. Phys.* **1985**, *82*, 284; Hay, P. J.; Wadt, W. R. *J. Chem. Phys.* **1985**, *82*, 299.
(25) Manoharan, P. T.; Gray, H. B. *J. Am. Chem. Soc.* **1965**, *87*, 3340.
(26) Frisch, J. M.; Trucks, G. W.; Schlegel, H. B.; Gill, P. M. W.; Johnson, B. G.; Robb, M. A.; Cheeseman, J. R.; Keith, T.; Petersson, G. A.; Montgomery, J. A.; Raghavachari, K.; Al-Laham, M. A.; Zakrzewski, V. G.; Ortiz, J. V.; Foresman, J. B.; Cioslowski, J.; Stefanov, B. B.; Nanayakkara, A.; Challacombe, M.; Peng, C. Y.; Ayala, P. Y.; Chen, W.; Wong, M. W.; Andres, J. L.; Replogle, E. S.; Gomperts, R.; Martin, R. L.; Fox, D. J.; Binkley, J. S.; Defrees, D. J.; Baker, J.; Stewart, J. P.; Head-Gordon, M.; Gonzalez, C.; Pople, J. A. *Gaussian 94, Revision C.3*, Gaussian, Inc.: Pittsburgh, PA, 1995.
(27) Harrison, W. A. *Electronic Structure and the Properties of Solids*, Dover Publications Inc.: New York, 1989; Chapter 8.